

Remarks on wave propagation in an acoustic metamaterial modeled as a relaxed micromorphic continuum

Jendrik Voss^{1,2,*}, Gianluca Rizzi^{1,**}, Plastiras Demetriou^{1,***}, Patrizio Neff^{2,†}, and Angela Madeo^{1,‡}

¹ Institute for Structural Mechanics and Dynamics, Technical University Dortmund, August-Schmidt-Str. 8, 44227 Dortmund, Germany.

² Chair for Nonlinear Analysis and Modeling, University of Duisburg-Essen, Thea-Leymann-Str. 9, 45127 Essen, Germany

In order to describe elastic waves propagation in metamaterials, i.e. solids with heterogeneities or microstructure, it is necessary to consider non-local or higher-order models. The relaxed micromorphic model (RMM) proposed here can describe these effects as a continuous material with enriched kinematics. We present a new unit cell giving rise to a metamaterial for acoustic application. The microstructure is engineered to show a band-gap in the low acoustic regime (600-2000 Hz) for which waves cannot propagate through the material. We concentrate on the size effects to make full advantage of the particularly beneficial structure that the model provides. The RMM material parameters are fitted using a new algorithm relying on cutoffs and asymptotes (obtained via a Bloch-Floquet analysis). In particular, by enhancing the kinetic energy of the model with a new inertia term, we enable decreasing curves (modes with negative group velocity).

© 2023 (copyright holder)

1 Introduction

Metamaterials are materials with heterogeneous microstructure whose mechanical properties go beyond those of classical materials. They can show various unusual static/dynamic responses and we will focus on the so-called band-gap phenomena [6, 14, 3, 4].

The direct finite element modeling of structures with its interior geometry is often unfeasible due to the extremely tight meshing that would be needed to correctly cover the interior microstructure. Thus, in actual engineering designs, a homogenized model with enriched kinematics to approximate the metamaterial's finite-size behavior is needed.

We propose to use an inertia-augmented relaxed micromorphic model. This model is based on the static relaxed micromorphic model [9, 8, 5] involving an additional macroscopic displacement field $P \in \mathbb{R}^{3 \times 3}$ and has been augmented with additional inertia terms accounting for coupled space-time derivatives of the micro-distortion tensor [1, 2, 10, 11, 12]. In this work, we present a guideline for the fitting procedure of this relaxed micromorphic model.

1.1 A metamaterial for acoustic control

The unit cell we use here is designed for acoustic control achieving a band-gap at relatively low frequencies (600 – 2000 Hz). This is obtained using polyethylene as a relatively soft base-material giving rise to lower wave speeds compared to aluminum, titanium, and other metals. Further, the adoption of a labyrinth-type geometry, cf. Figure 1, consisting of a circular center connected by thin bars, allows enabling local resonance phenomena of relatively low frequencies.

* Corresponding author, email: jendrik.voss@tu-dortmund.de

** email: gianluca.rizzi@tu-dortmund.de

*** email: plastiras.demetriou@tu-dortmund.de

† email: patrizio.neff@uni-due.de

‡ email: angela.madeo@tu-dortmund.de

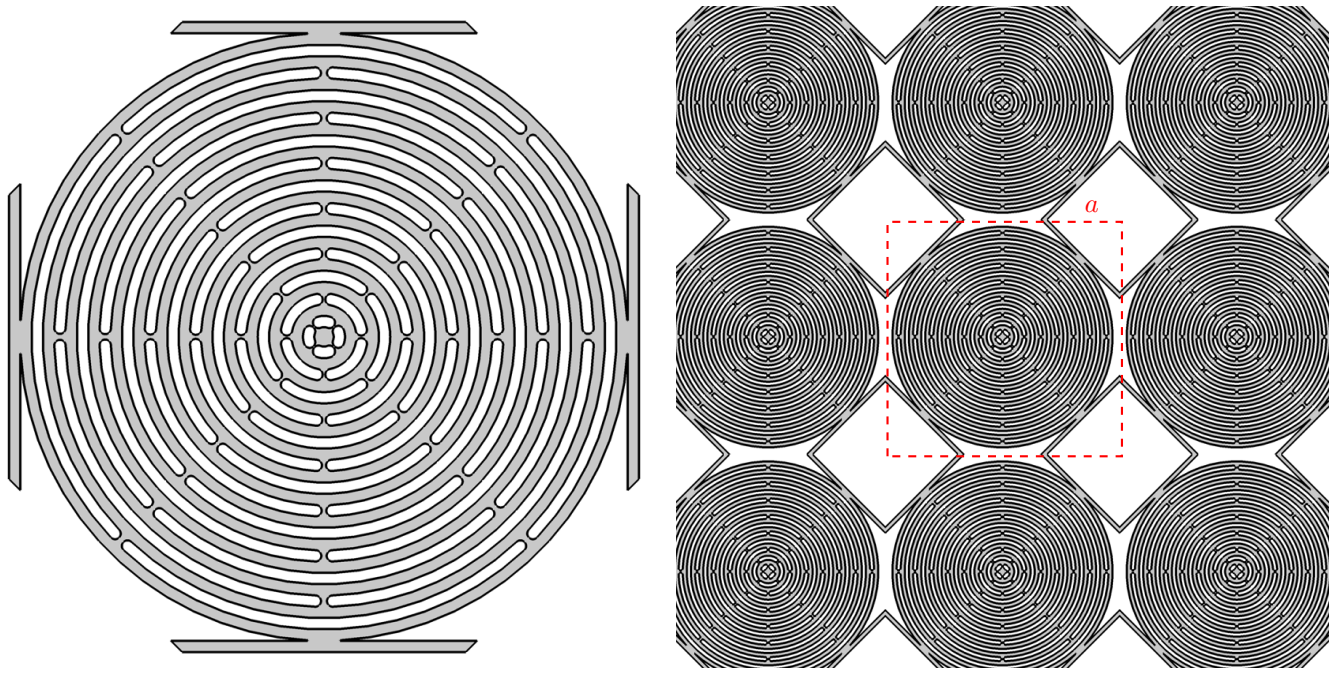


Fig. 1: Geometry of the unit cell. Left: details of one unit cell (rotated by 45 degrees) showing the tetragonal symmetry. For $a = 20\text{mm}$ as the size of the unit size we consider later, both the bars and holes have a thickness of 0.4mm each. Right: A 3×3 section of the metamaterial made up of this unit cell (red dashed square) showing how the cells are connected.

2 Relaxed micromorphic modelling of finite-size metamaterials

The Lagrangian \mathcal{L}_m for the relaxed micromorphic model enhanced with the additional micro-inertia term $\text{Curl } \dot{P}$ is [1, 2, 10, 11]

$$\mathcal{L}_m(\dot{u}, \nabla \dot{u}, \dot{P}, \text{Curl } \dot{P}, \nabla u, P, \text{Curl } P) = \underbrace{W(\nabla u, P, \text{Curl } P)}_{\text{strain energy}} - \underbrace{J(\dot{u}, \nabla \dot{u}, \dot{P}, \text{Curl } \dot{P})}_{\text{kinetic energy}}, \quad (1)$$

$$\begin{aligned} W(\nabla u, P, \text{Curl } P) &= \frac{1}{2} \langle \mathbb{C}_e \text{sym}(\nabla u - P), \text{sym}(\nabla u - P) \rangle \\ &+ \frac{1}{2} \langle \mathbb{C}_c \text{skew}(\nabla u - P), \text{skew}(\nabla u - P) \rangle + \frac{1}{2} \langle \mathbb{C}_{\text{micro}} \text{sym } P, \text{sym } P \rangle \\ &+ \frac{1}{2} \langle \mathbb{L}_s \text{sym } \text{Curl } P, \text{sym } \text{Curl } P \rangle + \frac{1}{2} \langle \mathbb{L}_a \text{skew } \text{Curl } P, \text{skew } \text{Curl } P \rangle, \end{aligned} \quad (2)$$

$$\begin{aligned} J(\dot{u}, \nabla \dot{u}, \dot{P}, \text{Curl } \dot{P}) &= \frac{1}{2} \rho \|\dot{u}\|^2 + \frac{1}{2} \langle \mathbb{J}_m \text{sym } \dot{P}, \text{sym } \dot{P} \rangle + \langle \mathbb{J}_c \text{skew } \dot{P}, \text{skew } \dot{P} \rangle \\ &+ \frac{1}{2} \langle \mathbb{T}_e \text{sym } \nabla \dot{u}, \text{sym } \nabla \dot{u} \rangle + \frac{1}{2} \langle \mathbb{T}_c \text{skew } \nabla \dot{u}, \text{skew } \nabla \dot{u} \rangle \\ &+ \frac{1}{2} \langle \mathbb{M}_s \text{sym } \text{Curl } \dot{P}, \text{sym } \text{Curl } \dot{P} \rangle + \frac{1}{2} \langle \mathbb{M}_a \text{skew } \text{Curl } \dot{P}, \text{skew } \text{Curl } \dot{P} \rangle \end{aligned} \quad (3)$$

where $u \in \mathbb{R}^3$ is the macroscopic displacement field, $P \in \mathbb{R}^{3 \times 3}$ is the non-symmetric micro-distortion tensor, ρ is the macroscopic apparent density, $\mathbb{J}_m, \mathbb{J}_c, \mathbb{T}_e, \mathbb{T}_c, \mathbb{M}_s, \mathbb{M}_a$, are 4th order micro-inertia tensors, and $\mathbb{C}_e, \mathbb{C}_c, \mathbb{C}_{\text{micro}}, \mathbb{L}_s$, and \mathbb{L}_a are 4th order elastic tensors. In absence of external body loads, we have the following equilibrium equation [10, 2, 9]

$$\rho \ddot{u} - \text{Div } \hat{\sigma} = \text{Div } \tilde{\sigma}, \quad \tilde{\sigma} = \tilde{\sigma} - s - \text{Curl } m - \text{Curl } \tilde{m}, \quad (4)$$

where we set

$$\begin{aligned} \tilde{\sigma} &:= \mathbb{C}_e \text{sym}(\nabla u - P) + \mathbb{C}_c \text{skew}(\nabla u - P) & \hat{\sigma} &:= \mathbb{T}_e \text{sym } \nabla \dot{u} + \mathbb{T}_c \text{skew } \nabla \dot{u}, \\ \tilde{\sigma} &:= \mathbb{J}_m \text{sym } \dot{P} + \mathbb{J}_c \text{skew } \dot{P}, & s &:= \mathbb{C}_{\text{micro}} \text{sym } P, \\ m &:= \mathbb{L}_s \text{sym } \text{Curl } P + \mathbb{L}_a \text{skew } \text{Curl } P, & \tilde{m} &:= \mathbb{M}_s \text{sym } \text{Curl } \dot{P} + \mathbb{M}_a \text{skew } \text{Curl } \dot{P}. \end{aligned} \quad (5)$$

3 Dispersion curves

We use the dynamic material’s behavior by considering elastic waves as the basis to fit the parameters of the relaxed micromorphic model. Thereby, the model’s consistency is checked against a standard Bloch-Floquet analysis of the wave propagation performed using the unit cell described in Figure 1 with built-in periodic Bloch-Floquet boundary conditions from *Comsol Multiphysics*[®]. We highlight the key points of the fitting procedure in the blue shaded boxes below.

The most general three-dimensional case results in an unmanageable amount of independent parameters for the relaxed micromorphic model. Here, we focus on a simpler setting:

1. We consider a plane strain ansatz, i.e. the components of u and P depend only on $\{x_1, x_2\}$ with vanishing out-of-plane components $u_3 = P_{13} = P_{31} = P_{23} = P_{32} = P_{33} = 0$.
2. We consider a tetragonal symmetry for the geometry of the unit cell and thus for all elastic and micro-inertia tensors of the relaxed micromorphic model.

The time harmonic ansatz for the components v_j of the displacement u and the micro-distortion tensor P is

$$v_j = \Psi_j e^{i(k_1 x_1 + k_2 x_2 - \omega t)}, \tag{6}$$

where Ψ_j is a scalar amplitude, $(k_1, k_2)^T = k(\sin \phi, \cos \phi)^T$ represents the wavevector with ϕ as the angle giving the direction of propagation, k the wave vector length, and ω is the frequency.

Substituting the ansatz (6) in the equilibrium equations (4), we obtain the homogeneous algebraic linear system

$$A\Psi = 0, \tag{7}$$

where $A = A(\omega, k, \phi) \in \mathbb{C}^{6 \times 6}$ is the *acoustic tensor* which depends on the frequency ω , the wave vector length k , the angle of propagation ϕ and all the constitutive parameters of the relaxed micromorphic model. The non-trivial solutions of the system (7) are obtained when A is singular, i.e. when $\det A = 0$, which provides relations between $\omega = \omega(k, \phi)$ (or $k = k(\omega, \phi)$), the so-called *dispersion relations*.

Aligning the angle of incidence ϕ with a symmetry axis of the unit cell’s geometry simplifies

$$\det A = p(k^2, k^4, k^6, k^8, \omega^2, \omega^4, \omega^6, \omega^8, \omega^{10}, \omega^{12}) = p_1(k^2, k^4, \omega^2, \omega^4, \omega^6) p_2(k^2, k^4, \omega^2, \omega^4, \omega^6), \tag{8}$$

where p_1 and p_2 are independent dispersion polynomials for shear and pressure waves, respectively.

3. We assume a 0° or 45° angle of incidence for the fitting procedure.

To avoid repeating the time-consuming fitting procedure when changing the size of the cell and the base material’s properties while keeping the geometry of the unit cell, we emphasize the following two observations from the Bloch-Floquet analysis with *Comsol Multiphysics*[®]:

- The dispersion curves scale inversely in both ω and k with respect to the size a of the unit cell.
- The dispersion curves scale proportionally in ω with respect to the speed of the wave of the bulk material composing the unit cell;

We can show the same invariance properties¹ analytically for the relaxed micromorphic model

$$L_c \rightarrow tL_c \implies p(\omega, k) \rightarrow \frac{1}{t^2} p(t\omega, tk), \tag{9}$$

$$\begin{matrix} (\mathbb{C}_e, \mathbb{C}_c, \mathbb{C}_{\text{micro}}, \mathbb{L}_s, \mathbb{L}_a) \\ \rho \rightarrow b\rho \end{matrix} \rightarrow a(\mathbb{C}_e, \mathbb{C}_c, \mathbb{C}_{\text{micro}}, \mathbb{L}_s, \mathbb{L}_a) \implies p(\omega, k) \rightarrow a^3 p\left(\sqrt{\frac{b}{a}} \omega, k\right). \tag{10}$$

¹ The scaling properties can have this simple shape by collecting an additional ρ and L_c^2 in front of all micro-inertia tensors [13].

4 Fitting of the relaxed micromorphic parameters

Overall, the relaxed micromorphic model has 19 parameters² in the plane strain tetragonal symmetry case

$$\rho, L_c, \mathbb{C}_{\text{micro}} \sim \{\kappa_m, \mu_m, \mu_m^*\}, \mathbb{C}_c \sim \{\mu_c\}, \mathbb{C}_e \sim \{\kappa_e, \mu_e, \mu_e^*\}, \mathbb{L}_s, \mathbb{L}_a \sim \{\alpha_1\}, \quad (11)$$

$$\mathbb{J}_m \sim \{\kappa_\gamma, \gamma_1, \gamma_1^*\}, \mathbb{J}_c \sim \{\gamma_2\}, \mathbb{T}_e \sim \{\bar{\kappa}_\gamma, \bar{\gamma}_1, \bar{\gamma}_1^*\}, \mathbb{T}_c \sim \{\bar{\gamma}_2\}, \mathbb{M}_s, \mathbb{M}_a \sim \{\beta_1\}. \quad (12)$$

We present an efficient automatic fitting procedure relying exclusively on the data from the Bloch-Floquet analysis done with *Comsol Multiphysics*[®]:

4. We set the characteristic length $L_c = a$ equal the size of the unit cell, cf eq. (9), and compute the macroscopic apparent density ρ as the product of the base material's density times the unit cells area percentage.

We can compute the parameters of the meso-scale \mathbb{C}_e depending on the micro-parameters $\mathbb{C}_{\text{micro}}$ and a new set of macro-parameters $\mathbb{C}_{\text{macro}}$ with the same structure [5, 7, 10]

$$\mathbb{C}_e = \mathbb{C}_{\text{micro}} (\mathbb{C}_{\text{micro}} - \mathbb{C}_{\text{macro}})^{-1} \mathbb{C}_{\text{macro}}, \quad \rightarrow \quad \mu_e = \frac{\mu_m \mu_M}{\mu_m - \mu_M}, \quad \kappa_e = \frac{\kappa_m \kappa_M}{\kappa_m - \kappa_M}, \quad \mu_e^* = \frac{\mu_m^* \mu_M^*}{\mu_m^* - \mu_M^*}. \quad (13)$$

In the limit of infinitesimal small unit-cells or rather of an indefinitely large body, these macro-parameters are obtained as the homogenization to a classical anisotropic Cauchy material [5, 7]

$$c_p = \sqrt{\frac{\kappa_M + \mu_M}{\rho}}, \quad c_s = \sqrt{\frac{\mu_M^*}{\rho}}, \quad \bar{c}_p = \sqrt{\frac{\kappa_M + \mu_M^*}{\rho}}, \quad \bar{c}_s = \sqrt{\frac{\mu_M}{\rho}}, \quad (14)$$

where c_p, c_s are the speed of pressure and shear wave, respectively, for 0° of incidence while \bar{c}_p, \bar{c}_s describe an incidence angle of 45° . The numerical values can directly be obtained by the slope of the acoustic curves at the origin $k = 0$.

5. We fit the macro parameters κ_M, μ_M, μ_M^* by the slope of the corresponding acoustic dispersion curves

$$\mu_M = \bar{c}_s^2 \rho, \quad \mu_M^* = c_s^2 \rho, \quad \kappa_M = (c_p^2 - \bar{c}_s^2) \rho = (\bar{c}_p^2 - c_s^2) \rho. \quad (15)$$

The cut-offs of the dispersion curves describe the frequency of the (higher) optic modes at $k = 0$ and play an important role in fitting the material parameters of the relaxed micromorphic model [7, 5, 10]. They allow for a simplified analytical expression of the roots of the dispersion polynomial as shown in Table 1 with

$$\omega_r = \sqrt{\frac{\mu_c}{\rho L_c^2 \gamma_2}}, \quad \omega_s = \sqrt{\frac{\mu_e + \mu_m}{\rho L_c^2 \gamma_1}}, \quad \omega_{ss} = \sqrt{\frac{\mu_e^* + \mu_m^*}{\rho L_c^2 \gamma_1^*}}, \quad \omega_p = \sqrt{\frac{\kappa_e + \kappa_m}{\rho L_c^2 \kappa_\gamma}}. \quad (16)$$

	0°	45°		0°	45°
shear	$\omega_2 = \omega_{ss}$	$\omega_2 = \omega_s$	pressure	$\omega_2 = \omega_s$	$\omega_2 = \omega_{ss}$
	$\omega_3 = \omega_r$	$\omega_3 = \omega_r$		$\omega_3 = \omega_p$	$\omega_3 = \omega_p$

Table 1: Cut-offs expressions for the pressure waves (left) and for the shear waves (right). The expressions ω_s and ω_{ss} change from pressure to shear and shear to pressure, respectively, when going from 0 to 45 degrees of incidence.

6. We write the micro-inertia parameters $\kappa_\gamma, \gamma_1, \gamma_1^*, \gamma_2$ as a function of the remaining elastic material parameters and the numerical values of the cut-offs

$$\kappa_\gamma = \frac{\kappa_e + \kappa_m}{\rho L_c^2 \omega_p^2}, \quad \gamma_1 = \frac{\mu_e + \mu_m}{\rho L_c^2 \omega_s^2}, \quad \gamma_1^* = \frac{\mu_e^* + \mu_m^*}{\rho L_c^2 \omega_{ss}^2}, \quad \gamma_2 = \frac{\mu_c}{\rho L_c^2 \omega_r^2}. \quad (17)$$

² We write “m” for “micro” and “M” for “macro” for the corresponding elastic parameters to shorten the following expressions.

We remain with 10 independent parameters $\kappa_m, \mu_m, \mu_m^*, \mu_c, \bar{\kappa}_\gamma, \bar{\gamma}_1, \bar{\gamma}_1^*, \bar{\gamma}_2, \alpha_1, \beta_1$. The analytical expressions of the dispersion curves, i.e. the roots of the dispersion polynomial (8), are unmanageable which makes it impossible to find further analytic identification of more parameters. Therefore, one is usually left with a very computationally heavy numerical minimization (we use *Mathematica*) to find the remaining material parameters. Here, we show a much faster alternative semi-analytical approach.

We consider the asymptotes ($k \rightarrow \infty$) of all dispersion curves (6 values each for 0° and 45°). The limit allows for simplified analytical expressions because we can omit terms of the dispersion polynomial which are of lower order in k and thus, we obtain simpler roots. However, in contrast to the analytical expression of the cut-offs (16), the asymptotes' expressions are still very large and cannot be shown here. This is mainly due to the fact that we must solve a full third-order polynomial while we only had two non-zero cut-offs each before.

7. We fit the remaining 10 parameters $\kappa_m, \mu_m, \mu_m^*, \mu_c, \bar{\kappa}_\gamma, \bar{\gamma}_1, \bar{\gamma}_1^*, \bar{\gamma}_2, \alpha_1, \beta_1$ by minimizing the mean square error of the asymptotes' expressions and the numerical values obtained via Bloch-Floquet analysis of the periodicity limit $k = \frac{1}{2L_c}$.

4.1 Results

The fitting shown in Figure 2 behaves well for all frequencies ω and wavenumber k for 0° of incidence but loses some precision for an incidence angle of 45° . The achieved overall precision allows us to explore the dispersive metamaterial's characteristics at a satisfactory level. We want to emphasize that we only fixed the dispersion curves at $k = 0$ and in the limit $k \rightarrow \infty$, the well-behaving shape in-between is an automatic result of the relaxed micromorphic model. In particular, with the additional micro-inertia term $\text{Curl } \dot{P}$, we can fit a dispersion curve with negative group velocity perfectly, the lower optic pressure curve for 45° , for the first time.

The fitting of the curves below the band-gap is not perfect due to the degenerated structure of $\text{Curl } \dot{P}$ and $\text{Curl } P$ in a plane problem [13], resulting in an isotropic behavior with only a single independent parameter α_1, β_1 each. This causes four asymptotes of the relaxed micromorphic model to coincide.

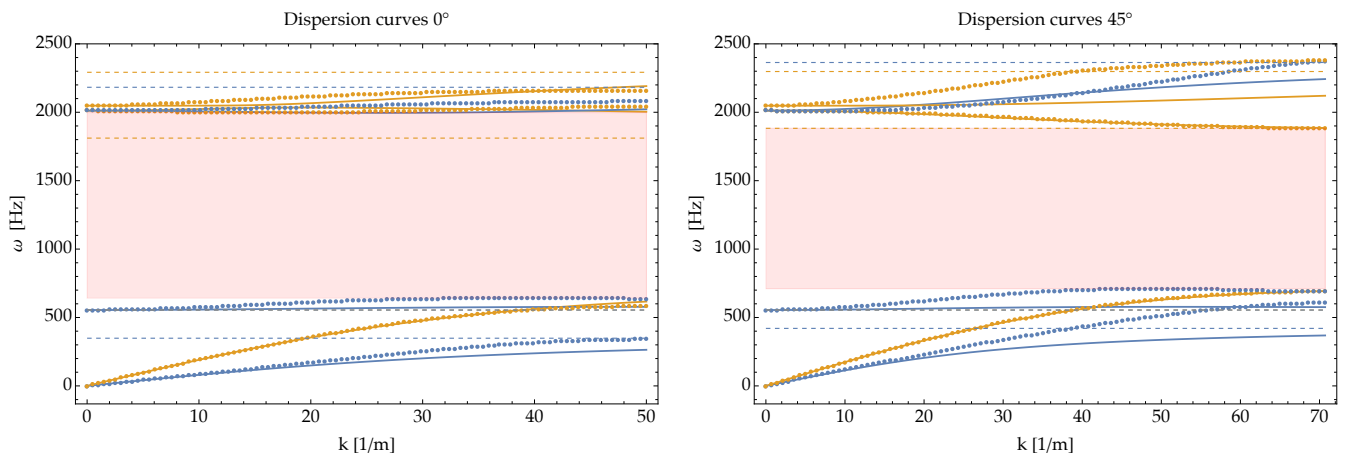


Fig. 2: Dispersion curves $\omega(k)$ for 0 degrees (left) and 45 degrees (right) with pressure curves colored in yellow and shear in blue. The dots are the points computed with *Comsol Multiphysics*® while the smooth curves show the analytical expression of the dispersion curves for the relaxed micromorphic model with an enhanced kinetic energy. The horizontal dashed lines show the asymptotes of the latter.

8. We can change the unit cell's size and its base material properties afterward: The scaling follows rule (9), i.e. we must change the characteristic length L_c to the new unit size a , and rule (10), i.e. we scale all elastic parameters of the relaxed micromorphic model $C_e, C_c, C_{\text{micro}}, L_s, L_a$ as well as the macroscopic apparent density ρ in consistency to the change in the unit cell's bulk material properties.

Acknowledgements Open access funding enabled and organized by Projekt DEAL.

References

- [1] A. Aivaliotis, A. Daouadji, G. Barbagallo, D. Tallarico, P. Neff, and A. Madeo. “Microstructure-related Stoneley waves and their effect on the scattering properties of a 2D Cauchy/relaxed-micromorphic interface”. *Wave Motion* 90 (2019). Pp. 99–120.
- [2] A. Aivaliotis, D. Tallarico, M.-V. d’Agostino, A. Daouadji, P. Neff, and A. Madeo. “Frequency- and angle-dependent scattering of a finite-sized meta-structure via the relaxed micromorphic model”. *Archive of Applied Mechanics* 90.5 (2020). Pp. 1073–1096.
- [3] O. R. Bilal, D. Ballagi, and C. Daraio. “Architected lattices for simultaneous broadband attenuation of airborne sound and mechanical vibrations in all directions”. *Physical Review Applied* 10.5 (2018).
- [4] P. Celli, B. Yousefzadeh, C. Daraio, and S. Gonella. “Bandgap widening by disorder in rainbow metamaterials”. *Applied Physics Letters* 114.9 (2019).
- [5] M. V. d’Agostino, G. Barbagallo, I.-D. Ghiba, B. Eidel, P. Neff, and A. Madeo. “Effective description of anisotropic wave dispersion in mechanical band-gap metamaterials via the relaxed micromorphic model”. *Journal of Elasticity* 139.2 (2020). Pp. 299–329.
- [6] Z. Liu, X. Zhang, Y. Mao, Y. Zhu, Z. Yang, C. T. Chan, and P. Sheng. “Locally resonant sonic materials”. *Science* 289.5485 (2000). Pp. 1734–1736.
- [7] P. Neff, B. Eidel, M. V. d’Agostino, and A. Madeo. “Identification of scale-independent material parameters in the relaxed micromorphic model through model-adapted first order homogenization”. *Journal of Elasticity* 139.2 (2020). Pp. 269–298.
- [8] P. Neff, I.-D. Ghiba, M. Lazar, and A. Madeo. “The relaxed linear micromorphic continuum: well-posedness of the static problem and relations to the gauge theory of dislocations”. *Quarterly Journal of Mechanics and Applied Mathematics* 68.1 (2015). Pp. 53–84.
- [9] P. Neff, I.-D. Ghiba, A. Madeo, L. Placidi, and G. Rosi. “A unifying perspective: the relaxed linear micromorphic continuum”. *Continuum Mechanics and Thermodynamics* 26.5 (2014). Pp. 639–681.
- [10] G. Rizzi, M. Collet, F. Demore, B. Eidel, P. Neff, and A. Madeo. “Exploring metamaterials’ structures through the relaxed micromorphic model: switching an acoustic screen into an acoustic absorber”. *Frontiers in Materials* 7 (2021). P. 589701.
- [11] G. Rizzi, M. V. d’Agostino, P. Neff, and A. Madeo. “Boundary and interface conditions in the relaxed micromorphic model: Exploring finite-size metastructures for elastic wave control”. *Mathematics and Mechanics of Solids* 27.6 (2022). Pp. 1053–1068.
- [12] G. Rizzi, P. Neff, and A. Madeo. “Metamaterial shields for inner protection and outer tuning through a relaxed micromorphic approach”. *arXiv preprint arXiv:2111.12001* (2021).
- [13] J. Voss, G. Rizzi, P. Neff, and A. Madeo. “Modeling a labyrinthine acoustic metamaterial through an inertia-augmented relaxed micromorphic approach”. *arXiv preprint arXiv:2204.02056* (2022).
- [14] P. Wang, F. Casadei, S. Shan, J. C. Weaver, and K. Bertoldi. “Harnessing buckling to design tunable locally resonant acoustic metamaterials”. *Physical Review Letters* 113.1 (2014).